

# Intramolecular Complexation in Aqueous Solutions of an End-Capped Poly(Ethylene Glycol)

G. Cojocariu\* and A. Natansohn†

Department of Chemistry, Queen's University, Kingston, Ontario, K7L 3N6, Canada

Received: December 6, 2001; In Final Form: April 3, 2002

$^1\text{H}$  NMR, 2D NOESY, and spin–lattice relaxation time ( $T_1$ ) measurements were used to investigate the aqueous solution behavior of poly(ethylene glycol) monomethyl ether 3,5-dinitrobenzoate (PEG-DNB). A cloud point diagram revealed a phase behavior consisting of two phase separation processes, one, at high temperature, common for solutes containing oxyethylene groups whose solubility in water decreases with temperature, and the other, at low temperature, driven by the hydrophobicity of the DNB group. The intramolecular charge-transfer complexation between the ether oxygens from the PEG chains, acting as p-electron donors, and the dinitrobenzoyl group, which is a  $\pi$ -electron acceptor, was found to be the cause of the unusual phase behavior and  $^1\text{H}$  NMR multiplet patterns. The molecular weight selectivity of the chemical shift was correlated to the different conformations adopted by complexes having different PEG lengths. These conformations are the result of the competition between hydration forces on one hand, and CT interactions and hydrophobicity of DNB on the other. In addition to complexation, there are large aggregates forming due to the amphiphilic character of these molecules. To explain the coexistence of aggregation and coiled complex conformation a model is proposed, consisting of supramicellar composite (multicenter) aggregates formed by the association of many PEG-DNB coils, each being unimolecular micelles. The composite aggregates are characterized by a hydrophobicity gradient associated with the molecular weight distribution along the aggregate radii.

## Introduction

Poly(ethyleneglycol) (PEG) attracts a lot of interest mainly due to properties deriving from its particular ability to develop various types of secondary interactions. Hydrogen bonding to water molecules have made PEGs some of the most investigated nonionic water-soluble polymers.<sup>1</sup> There are numerous studies about the molecular complexes formed by PEGs involving dipole–dipole interactions,<sup>2,3</sup> hydrogen-bonding<sup>4,5,6</sup> or coordination to alkali metal cations,<sup>7,8,9</sup> the latter being extensively investigated as polymer electrolytes in lithium-ion batteries.<sup>10</sup> Less attention was dedicated to the charge transfer (CT) complexation between PEG and aromatic  $\pi$ -electron acceptors, despite the interesting features observed for  $n$ - $\pi$  complexes formed by other polyethers such as crown-ethers<sup>11</sup> or poly(vinyl methyl ether) that forms with poly(styrene) a miscible polymer blend.<sup>12</sup>

In the process of investigating a 3,5-dinitrobenzoyl end-capped poly(ethylene glycol) (PEG-DNB), we have noticed novel intramolecular CT interactions. Attaching a  $\pi$ -electron acceptor at the end of a PEG chain (that can act as a p-electron donor) is expected to induce some constraints on the polyether chain conformation. However, this relationship has to be mutual, any conformational perturbation of the polymer chains would affect the strength of the CT complex. The significant changes in chemical shift that are associated with CT interactions make NMR a very efficient tool in investigating this class of complexes.<sup>13</sup> We have reported previously<sup>14</sup> very unusual multiplet patterns in the  $^1\text{H}$  NMR spectra of PEG-DNB solutions in  $\text{D}_2\text{O}$ , at concentrations higher than about 4 wt. %. The methyl and the aromatic signals were split each in about twelve peaks,

which was the number of oligomers detected by GPC. These multiplet patterns were the result of the weight polydispersity of the PEG chains.<sup>14</sup> The conformation of CT complexes formed between the ether oxygen atoms and the DNB ring is very sensitive to the length of the polyether chain, giving rise to chemical shift resolution by molecular weight. From the intensity of the peaks in the methyl multiplet we were able to obtain a molecular weight distribution curve in good agreement with the one given by GPC. In this paper, we try to elucidate the molecular mechanism responsible for this oligomer resolution.<sup>14</sup> The interpretation of the unusual  $^1\text{H}$  NMR behavior considers the two main phenomena that occur simultaneously in concentrated aqueous solutions: CT complexation between PEG and DNB, and the aggregation induced by the amphiphilic character of PEG-DNB molecules. A model that accounts for the observed behavior in aqueous solution of PEG-DNB is presented.

## Experimental Section

**Materials.** The synthesis of monomethyl ether poly(ethylene glycol) 3,5-dinitrobenzoate (PEG-DNB) was described previously.<sup>14</sup>

**NMR.**  $^1\text{H}$  NMR, 2D NOESY, and  $T_1$  spin–lattice relaxation time constants were recorded at  $298.0 \pm 0.1$  K, unless otherwise specified, with a variable temperature 5 mm Bruker BBI probe installed on an AVANCE–400 spectrometer. The solvents used were  $\text{D}_2\text{O}$  or  $\text{CDCl}_3$ . For the aqueous solutions, 2,2,3,3-d(4)-3-(trimethylsilyl)propionic acid sodium salt (concentration of about 50 ppm) was used as internal reference. The solutions, except the phase separated ones, were filtered through Millipore microsyringe filters, having a porosity of  $0.25 \mu\text{m}$ , directly into the NMR tubes. Degassing was done by freeze–thaw cycling under vacuum. After 3 to 5 cycles, there were no more gas bubbles coming out during the thaw. The sealed tubes were stored for at least a week for equilibration before any measure-

\* To whom correspondence should be addressed. E-mail: Gheorghe.Cojocariu@gepex.ge.com.

† Almeria Natansohn died on Sept. 10, 2002 after a long illness.

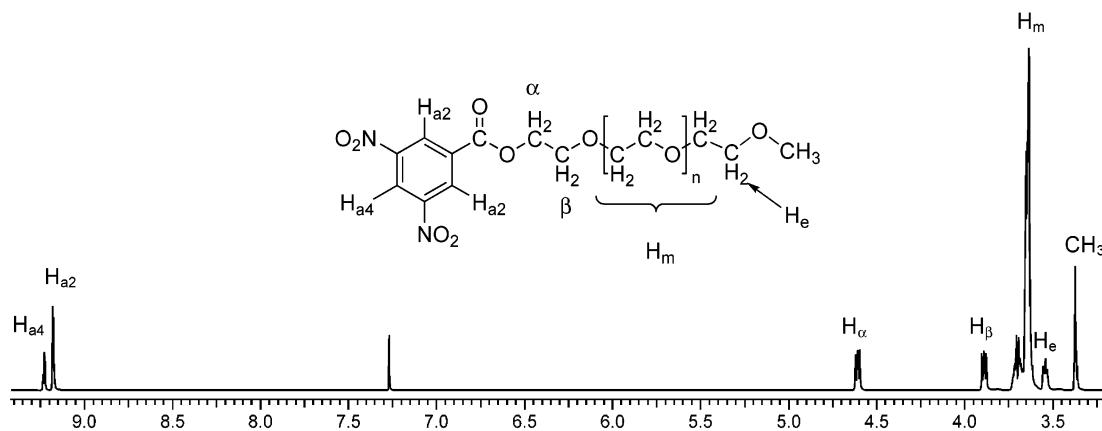


Figure 1.  $^1\text{H}$  NMR spectrum of PEG-DNB in  $\text{CDCl}_3$  and its assignments.

ment was done. 2D NOESY and EXSY experiments<sup>15,16</sup> were performed in the phase sensitive mode (TPPI),<sup>17</sup> typically using 2 K of memory for 512 increments. Mixing times between 0.1 and 1.5 s were used and maximum cross-peaks were obtained at 0.5 s. The spin lattice relaxation time constants were determined using a standard  $180-\tau-90$  inverse recovery pulse sequence<sup>18</sup> with  $>5T_1$  delay between pulse sequences allowing the spin system to relax to equilibrium. Ten  $\tau$  values between 0.01 and 30 s were applied and evaluated by the nonlinear curve fitting software of the spectrometer. The experimental error between duplicate experiments was less than 5%.

**Clouding Point Curves (CPC).** Above room temperature, the clouding points were observed visually while the solution temperature was increased stepwise, 1 °C at a time, using a thermoregulated bath. At each temperature, the solution was allowed about 30 min to equilibrate. For the data below room temperature, the same variable temperature probe employed for NMR was used. It was cooled by  $\text{N}_2$  gas flow. The same stepwise procedure was involved, but this time the NMR signal broadness was used as an indicator for phase separation, then confirmed by visual inspection. The temperature interval scanned was between  $-10$  °C and  $80$  °C.

**UV-vis Spectroscopy.** Electronic spectra were recorded on a Hewlett-Packard 8452A diode array ultraviolet-visible spectrophotometer, at room temperature. The samples were prepared in the same way as for NMR (except degassing) using the same deuterated solvents.

**Thermal Characterization.** Thermal transitions for the PEG-DNB and ethyl 3,5-dinitrobenzoate ester were detected with a Perkin-Elmer DSC 6 instrument, under nitrogen atmosphere, at a heating rate of  $5$  °C/min. The temperature range was from  $-100$  to  $300$  °C. The melting point of the white powder PEG-DNB was determined using a Fisher-Johns melting point apparatus at a heating rate of  $2$  °C/min.

## Results and Discussion

**Physical Properties and Phase Behavior.** Figure 1 shows the molecular structure of PEG-DNB and its  $^1\text{H}$  NMR spectrum in  $\text{CDCl}_3$ . The DNB group is a good  $\pi$ -electron acceptor, whereas the oxygen atoms from the polyether chain can act as p-electron donors.<sup>19</sup> This creates the possibility of CT interactions between the two parts of the molecule. Some of the physical properties of PEG-DNB are a direct consequence of these interactions. The compound purified by column chromatography is a reddish viscous liquid and its aqueous solution UV spectrum shows an absorption tail in the region  $400$ – $500$  nm (Figure 2). The only transition in the DSC thermogram between  $-150$  °C and  $300$  °C is the glass transition at about

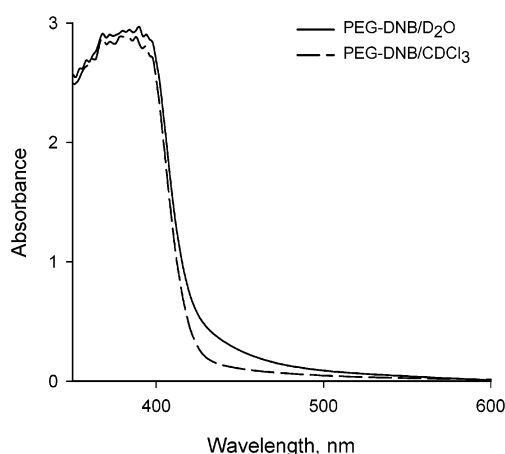


Figure 2. Electronic spectra of PEG-DNB in water and chloroform solutions having a concentration of  $0.123$  mol/L.

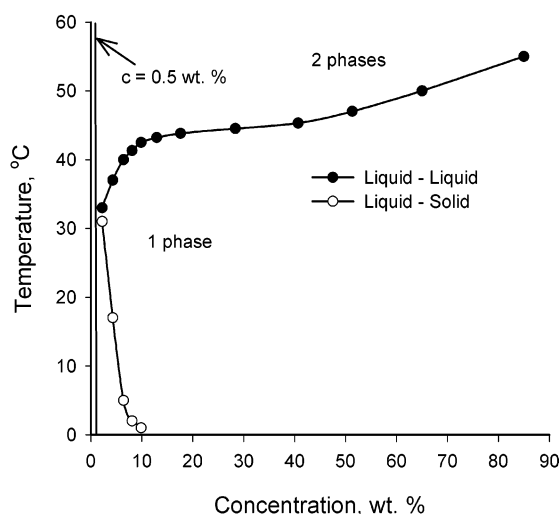
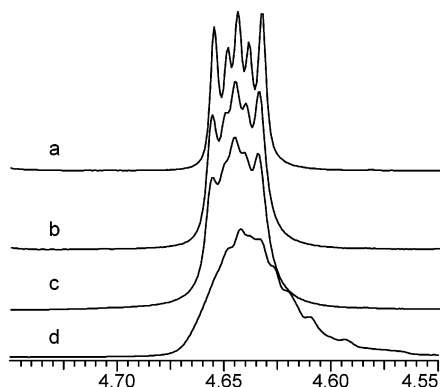


Figure 3. Clouding point curves (CPC) for the aqueous solutions of PEG-DNB.

$-57$  °C. The absence of any crystallization for PEG-DNB, as opposed to the poly(ethylene glycol) precursor that is crystalline at temperatures below  $-10$  °C, must be related to the fact that CT interactions would require the molecule to adopt a coil conformation, which may be impossible to accommodate into a crystalline lattice.

In Figure 3, a phase diagram obtained by clouding point curves (CPC) is presented. For concentrations smaller than  $0.5$  wt. % (marked by a vertical line) the solutions are clear and colorless. At room temperature, between  $0.5$  and  $2.2$  wt. % the



**Figure 4.** <sup>1</sup>H NMR spectrum in the region of the methylene next to DNB (CH<sub>2</sub> α) for aqueous solutions having: (a) 0.2, (b) 1.3, (c) 2.2, and (d) 4.3 wt. % PEG-DNB.

system is phase separated. For concentrations higher than 2.2 wt. %, a one-phase regime of clear and reddish solutions is bordered by two CPCs, an upper one corresponding to a liquid–liquid-phase separation, and a lower one describing a solid–liquid-phase separation. The upper clouding temperature is a common feature for aqueous solutions containing oxyethylene compounds, whose phase diagrams exhibit a lower critical solution temperature (LCST). To explain this phase separation, several mechanisms involving the hydrogen bonding between the ether oxygens and water,<sup>20</sup> the conformation of the PEG chain,<sup>21</sup> and the structure of the surrounding water<sup>22</sup> have been proposed. In the one phase regime above, the liquid–solid-phase separation, the solutions maintain a reddish color, suggesting the existence of CT complexes. As will be shown later, for this regime, <sup>1</sup>H NMR, and NOESY experiments support the hypothesis of CT complexes in which the oligoether is surrounding the hydrophobic group, shielding it from water.

When cooling the solution to the liquid–solid-phase separation temperature, hydrogen bonding between the ether oxygens and water becomes prevalent, and the PEG chain is pulled out, destroying the CT complex. This leaves the hydrophobic DNB group exposed to water, and the liquid–solid-phase separation occurs. Literature indicates that in aqueous PEG solutions, the –C–C– dihedral gauche conformer population increases with the amount of water, a maximum of almost 100% being reached at about 0.016 molar fraction of oxyethylene units.<sup>23–27</sup>

This molar fraction corresponds to about 5 wt. % PEG-DNB, close to the concentration of the liquid–solid-phase separation observed at room temperature. The high gauche population in dilute solutions is confirmed in our case by the NMR data. In Figure 4, the <sup>1</sup>H NMR for the methylene group, H<sub>α</sub>, next to the DNB ring, is shown. The dilute solutions (Figure 4a,b, and c) have a good resolution allowing for J-coupling measurements, while solutions having concentrations higher than 4 wt. % show featureless, highly overlapped, signals (Figure 4d) due to CT complexation. Considering that the methylene protons can be treated as an AA'XX' system,<sup>28</sup> the rotationally averaged J coupling constants are calculated to be  $J_{AX} = J_{A'X'} = 6.3$  Hz and  $J_{AX'} = J_{AX} = 2.5$  Hz. Using these values with the equations given by the Rotational Isomeric State (RIS) model,<sup>29</sup> the population of the gauche states for the EO unit next to DNB can be estimated at about 85 ± 9%, roughly the same for the three dilute solutions given in Figure 4. A similar calculation for the second EO unit produces an even more dominant population of gauche state, about 95 ± 5%.

The O···O distance, in a single oxyethylene unit in the gauche conformation (0.28–0.30 nm),<sup>30</sup> is very similar to the corre-

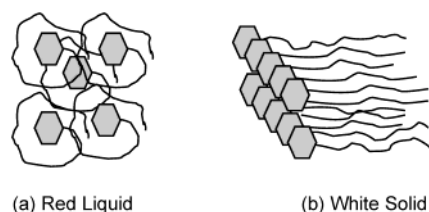


**Figure 5.** Schematic representation of the PEG-DNB conformation in liquid (a) and solid (b) state.

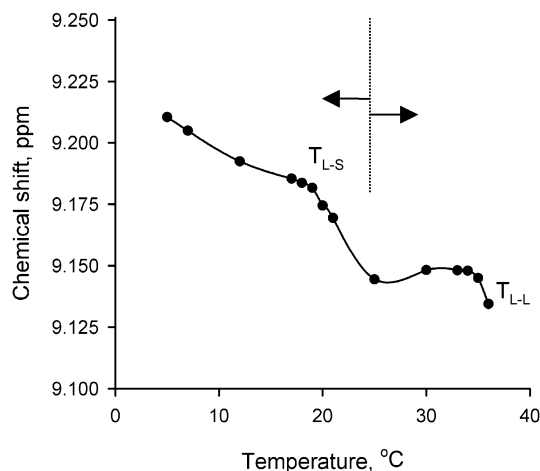


**Figure 6.** Temperature dependence of the chemical shift of DNB protons for an aqueous solution of 4.3 wt. % PEG-DNB. Chemical shift is read for the peak corresponding to the hepta(ethyleneglycol) fraction and is expressed as change from the value at 25 °C.

sponding distance (0.285 nm) in liquid water.<sup>31</sup> Therefore, the ether oxygens of PEG chains in the gauche conformation fit favorably in the water network contributing to the removal of the PEG chains from the CT complex and consequently to phase separation. This phase separation moves to higher concentrations as the temperature decreases (Figure 3), because at lower temperatures –C–C– gauche conformation<sup>32,33,34</sup> and hydrogen bonding<sup>20</sup> to water molecules are favored. Therefore, less water is needed to reach the critical concentration of gauche conformers that induces phase separation.

Another interesting aspect about the lower temperature phase separation is the fact that PEG-DNB precipitates as a white solid, whereas the purified compound is a red viscous liquid. The <sup>1</sup>H NMR of the white solid is similar with the spectrum of the initial PEG-DNB (Figure 1). Although in organic solvents and in concentrated aqueous solutions, the coil conformation is favored, in dilute aqueous solution the hydrogen bonding stretches the conformation to a point where a crystalline arrangement becomes possible. The van der Waals attraction between the decomplexed hydrophobic DNB rings may trigger crystallization. These specific conditions allow the formation of the white crystalline powder, which melts at 82–86 °C forming the same red viscous liquid that does not crystallize back on cooling. This proves that, after melting, the coiled complexes (Figure 5, a) reform and cannot fit into a crystalline lattice anymore. The melting temperature is not very different from the melting point measured for ethyl 3,5-dinitrobenzoate (90–92 °C) suggesting that the lattice energy comes mainly from the aromatic DNB stacking (Figure 5, b).

The above mechanism for phase separation is supported by the temperature dependence of the DNB protons chemical shift (Figure 6). Cooling the 4.3 wt. % solution down to 17 °C (the lower temperature phase separation in Figure 3) causes a sharp increase in the chemical shift of the DNB acceptor protons. This

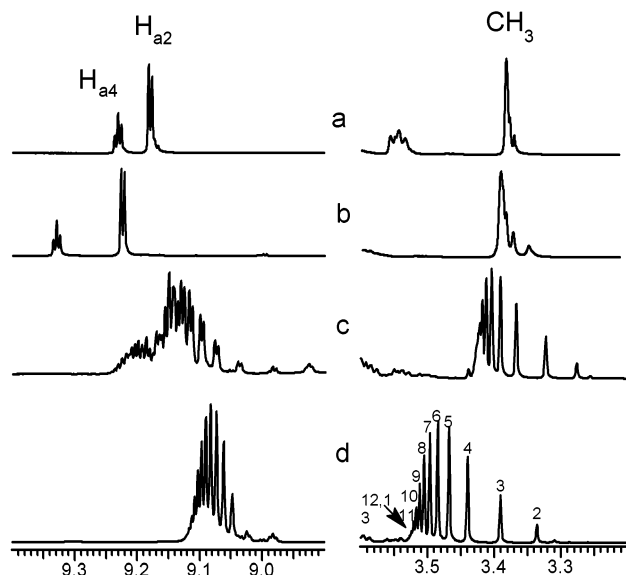


**Figure 7.**  $^1\text{H}$  NMR spectrum in the region of DNB (left) and methyl (right) for various solutions of PEG-DNB: (a) chloroform, 15.0 wt. %, (b)  $\text{D}_2\text{O}$ , 0.20 wt. %, (c)  $\text{D}_2\text{O}$ , 4.3 wt. %, and (d)  $\text{D}_2\text{O}$ , 15.0 wt. % (Numbers are EO units per PEG chain).

indicates a decrease in the electron density around these protons, confirming the CT decomplexation as a consequence of conformational stretching by the hydrogen bonding. When heating this solution above room temperature, just before reaching the liquid–liquid-phase separation temperature (36 °C), a decrease in the DNB chemical shift is noticed, which suggests strengthening of CT interactions. The conformational models<sup>21,33</sup> describing the high-temperature phase separation in oxyethylene compounds consider that, when the temperature is raised, the  $-\text{C}-\text{C}-$  gauche conformer population decreases significantly. This conformation change brings the ether oxygens in an orientation less favorable to water hydrogen bonding. The less hydrated PEG chains will collapse onto the DNB groups intensifying the CT interactions, as suggested by the increased DNB protons shielding in Figure 6.

**Multiplet Pattern.** The most peculiar feature of this molecule is found in its proton NMR spectra. The reddish solutions in the one-phase regime (Figure 3), show very uncommon multiplet patterns (Figure 7c and d) in contrast to the “normal” spectra observed in dilute aqueous solutions (Figure 7b) or in chloroform (Figure 7a). For example, the methyl signal, which is expected to be a singlet, consists of about twelve distinct peaks (Figure 7d) in the NMR measured in concentrated aqueous solutions. A similar multiplicity can be observed for the aromatic protons. This splitting is less obvious for the rest of the signals (not shown) due to substantial overlapping.

All the solutions that show the unusual splitting pattern are reddish in color and show NOESY cross-peaks between PEG and DNB protons ( $\text{H}_{\text{DNB}}$ ,  $\text{H}_m$ ) in Figure 8), indicating that the unusual NMR peaks must be related to the CT interactions that occur within this molecule (vide supra).

PEG is known to interact strongly with water molecules by hydrogen bonding,<sup>20</sup> whereas in chloroform weaker dipolar interactions are expected between the solvent and the solute. On the basis of that, one would actually expect that the competition between hydrogen bonding and CT interactions to produce weak complexes in aqueous solutions. Although this is true for dilute solutions, the NMR and UV data suggest that the strongest complexation exists in concentrated aqueous solutions, even stronger than in chloroform. The chloroform

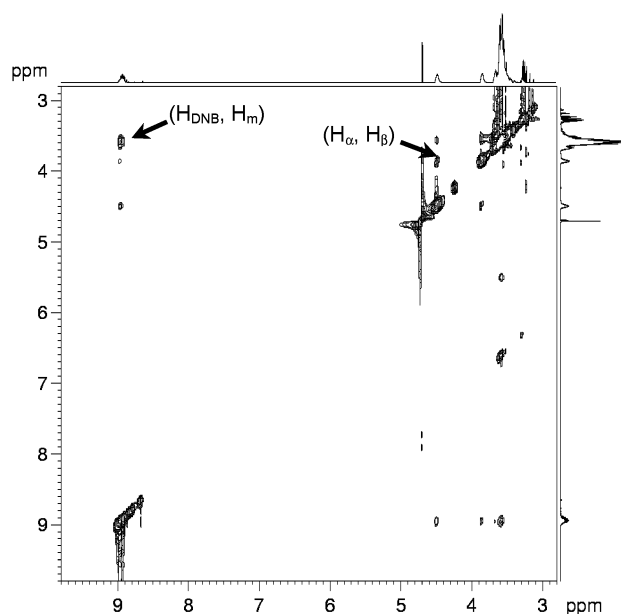


**Figure 8.** 2D NOESY spectrum for a solution of 6.3 wt. % PEG-DNB in  $\text{D}_2\text{O}$ . Mixing time is 0.5 s. The arrows point to the ( $\text{H}_{\text{DNB}}$ ,  $\text{H}_m$ ) and ( $\text{H}_\alpha$ ,  $\text{H}_\beta$ ) cross-peaks.

solutions do not show any splitting pattern or NOESY cross-peaks for a wide range of concentrations (0.1 to 30.0 wt. %). Furthermore, as can be seen in Figure 2, the UV absorbance in the 400–500 nm region is more intense in the aqueous solution than in the chloroform solution of the same concentration. The hydrophobic effect has to be considered as a probable factor. For example, solubilization of benzene and several benzene derivatives in dilute aqueous solutions of 18-crown-6 ether was reported to be due to weak hydrophobic interactions.<sup>35</sup> In the case shown here, the DNB group is more hydrophobic than the PEG chain, consequently the PEG will tend to coil around the DNB in water solutions to reduce the hydrophobic energy and will in this way provide conformations that are very favorable to CT interactions. The proximity of the PEG main chain and DNB is demonstrated by the 2D NOESY cross-peaks observed between the  $\text{H}_m$  peaks and the aromatic multiplet (Figure 8). In chloroform solutions, both PEG and DNB are soluble, therefore there is less driving force for the CT interactions. As shown in the previous section, in dilute aqueous solutions the hydrogen bonding overcomes both the hydrophobic effect and the CT interactions.

As previously<sup>14</sup> assigned, the peaks within the methyl multiplet correspond to oligomers having from 2 EO units (upfield) to about 12 EO units (downfield) in the PEG chain (Figure 7d). The same kind of assignment can be done for the aromatic peaks. The multiplet pattern is determined by the dependence of the PEG-DNB conformation on the length of the PEG chain, different conformations within the CT complex producing different chemical shifts for the protons involved. This molecular weight resolution could only be obtained if the observed molecular complexes were intramolecular in nature. Since the oligomers are expected to be randomly mixed in solution, the number of possible intermolecular complexes would be much larger than 12 and they would most likely produce a featureless broad signal.

The difference in chemical shift between molecules having different CT conformations is the result of the balance between three main types of interactions that can occur in this system: hydration, CT and ring current effects. CT complexation alone should cause shielding of the DNB acceptor protons and



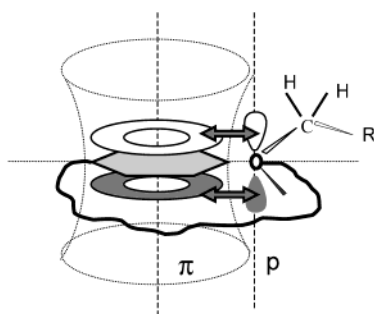


**Figure 9.** HOMO/LUMO interactions in  $n$ - $\pi$  complexes of ethers and aromatic rings. Ring currents shield the protons above/below the ring and deshield the protons in the ring plane.

deshielding of the ether protons due to the ether oxygens donating some of their electron density to the aromatic ring.<sup>13</sup> Depending on the geometry of the complex, the ring currents from the DNB group can affect the chemical shifts of the PEG protons.<sup>36</sup> Finally, the hydration of the PEG chain is expected to deshield the ether protons.<sup>37</sup> For the hydrophobic DNB, it is reasonable to assume that the main interaction altering the chemical shift is the transfer of electron density from the ether oxygens. The DNB protons appear more shielded in the molecules having shorter polyether chains, suggesting that the complexes they form are more compact than in the long-chained analogues. Less straightforward to analyze is the methyl multiplet, here all of the above-mentioned interactions could influence significantly the chemical shift. Comparing the spectra in Figure 7b and c, one can see that on complexation the methyl protons of the longer chains move downfield in comparison with the dilute sample, whereas for the short chains a significant shielding is noted. The shorter PEG, which should form tighter complexes, will have their methyl closer to the DNB group where the shielding caused by the ring currents should overcome the loss in electron density due to CT. It is also very likely that the PEG hydration will be less for the compact complexes. The longer chains place their methyl group farther from the ring, where, even if the electron density loss through CT is diminished, they will be significantly less shielded because of the drastic reduction of the ring currents when moving away from the ring.<sup>36</sup> Higher hydration for these chains probably also contributes to deshielding. For the shortest chains, the maximum shielding the methyl protons experience, in comparison to the dilute solution peak, is about 0.1 ppm. This, even when accounting for the electron density loss through CT, indicates that at the best the ring currents produce increases in shielding of the order of few tenths of ppm. Hence, it is very likely that the methyl groups are situated on the side of the DNB ring, slightly above its plane (Figure 9), where the ring currents are indeed weak.<sup>36</sup> The literature does not provide any hint for the geometry of  $n$ - $\pi$  complexes involving ethers and aromatic rings. The assumption made by Andrews and Keefer<sup>11</sup> about the ether oxygens lying above the plane of the acceptor ring is unlikely. The CT interactions are considered to be favored by maximum overlapping between the donor's HOMO and acceptor's LUMO.<sup>19</sup> Such an optimum orbital interaction between  $p$ -orbitals from oxygen and  $\pi$ -orbitals from the DNB ring should occur when the oxygen is situated on the side of the ring, in the ring's plane, and with the interacting  $p$ -orbital parallel to the C6 axis (Figure 9). This model is in agreement with the weak ring currents observed on CH<sub>3</sub> in this report.

So far, we demonstrated that the balance between the hydrophobic interactions, which favors complexation, and the hydration, that tends to remove the PEG chain away from the

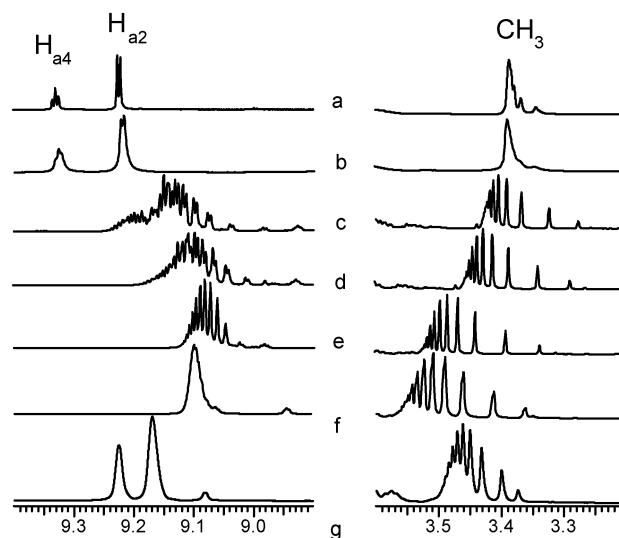


**Figure 10.** <sup>1</sup>H NMR of PEG-DNB/D<sub>2</sub>O solutions at different concentrations: (a) 0.3, (b) 2.2, (c) 4.3, (d) 6.3, (e) 15.0, (f) 51.3, and (g) 85.0 wt. %.

DNB, determines the conformation of the molecule. For the complexation of the molecules having shorter PEG chains, and consequently, a higher hydrophobe/hydrophile ratio, the hydrophobic interactions are dominant producing stronger CT interactions. For the more hydrophilic higher molecular weight PEG-DNBs, the longer the PEG chain, the stronger will be the stretching force exerted by hydration, and the weaker the CT interactions. Sound velocity and density measurements<sup>38</sup> showed that the interaction strength of the water molecules H-bonded to the EO oxygens increases with the length of the PEG chain, reaching a basically constant value for a degree of polymerization of about 10. This is in good agreement with our results.

**Concentration Effects.** The <sup>1</sup>H NMR spectra of concentrated aqueous solutions show features that change with concentration. The <sup>1</sup>H NMR spectra for the aromatics (left) and methyl (right) protons at different concentrations are presented in Figure 10. The dependence of the aromatic protons chemical shift on the concentration shows two regimes. Below about 15 wt. % (Figure 10, a to e), dilution causes the aromatic multiplet to shift downfield, suggesting that adding more water causes CT decomplexation of the DNB group. In this concentration regime, hydration of PEG is dominant, overcoming the CT interaction and the hydrophobic effect. When hydration is complete, the PEG chains are enclosed in a three-dimensional network formed by water molecules interconnected by hydrogen bonding.<sup>39</sup> To define the fully hydrated state one should know the hydration number, which is the number of water molecules associated with an ethylene oxide (EO) unit. The numbers reported in the literature cover a wide range: from 1 to 6 water molecules per EO unit.<sup>40,41</sup> The decomplexation, beginning at about 15 wt. % on dilution, is caused by the local formation of these hydrogen bonding networks that start pulling the PEG chain out of the CT complex. This concentration range corresponds to hydration numbers a bit higher than 6, consistent to what was previously determined by NMR.<sup>41</sup> The higher apparent hydration numbers found in our case are due to the less efficient hydration of the hydrophobically capped PEGs.

At concentrations higher than about 15 wt. % (Figure 10e–g), the opposite behavior is observed. Dilution causes more shielding of the DNB protons, suggesting more CT complexation. In this concentration range, the amount of water is not sufficient to form a hydrogen-bonded network that would include the EO units. Consequently, the stretching pressure

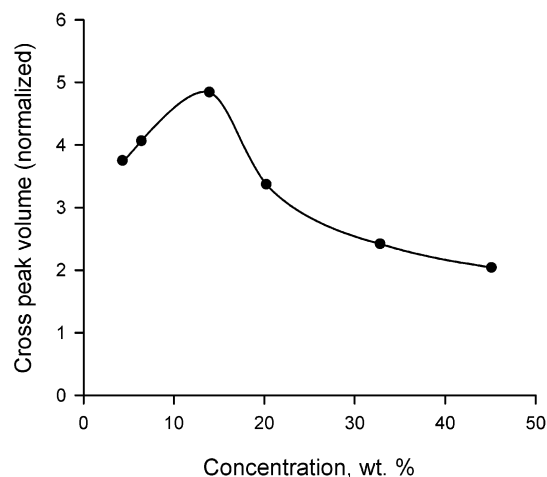


**Figure 11.** Volume of the 2D NOESY cross-peaks between DNB ( $H_{\alpha 2}$  and  $H_{\alpha 4}$ ) and PEG ( $H_m$ ) protons for aqueous solutions of PEG-DNB, normalized with respect to the ( $H_{\alpha}$ ,  $H_{\beta}$ ) cross-peak.

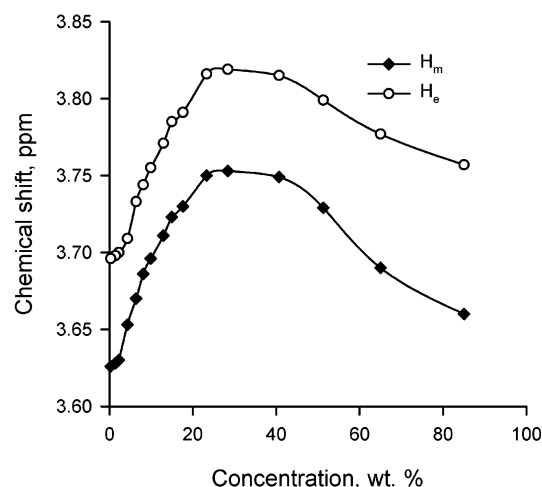
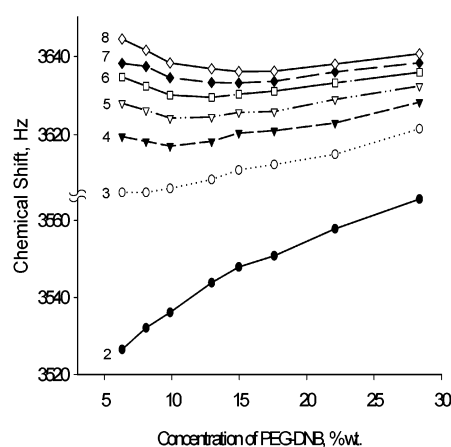


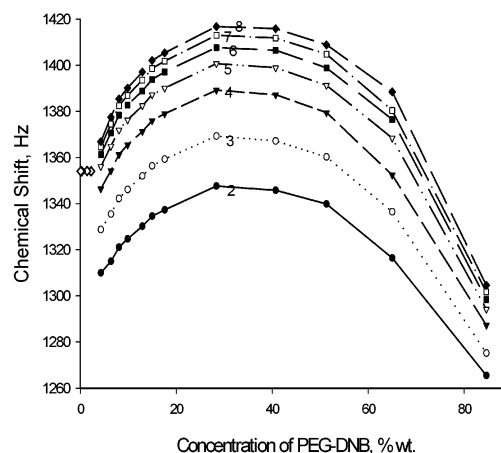
**Figure 12.** Concentration dependence for the chemical shift of the methylene protons ( $H_m$ ,  $H_e$ ).

exerted by the hydrogen bonds onto the PEG chains is not active, or is less intense, in concentrated samples. In these samples, the hydrophobic character of the DNB is dominant and causes the PEG chains to collapse onto the DNB group. This behavior is supported by the NOESY data shown in Figure 11, suggesting that the PEG chain is at its closest to the DNB group at concentrations of about 14 wt. %. The volume of the DNB/PEG cross-peaks was normalized by the volume of the cross-peak between the methylene groups of the EO unit next to DNB,  $H_{\alpha}$ , and  $H_{\beta}$  (Figure 8). In concentrated solutions, a spin diffusion contribution has to be taken into account. However, this means that the true NOEs at high concentration will be even smaller, which means that the trend displayed in Figure 11 is still valid.

In Figure 12 the methylene protons show the same trend with concentration as the methyl multiplet (Figure 10, right). The chemical shift of these protons supports the existence of the two regimes described above. In the high concentration regime, on dilution, all polyether protons move downfield. We already showed that in this regime dilution causes the PEG chain to collapse onto the hydrophobic DNB. The observed chemical shift change indicates that the hydration associated with dilution and the CT associated with the PEG collapse (both having deshielding effects on PEG protons) overcome the shielding caused by the increased ring currents effect. For the dilute regime, when fully hydrated, the PEG chains are being pulled



(a)



(b)

**Figure 13.** Concentration dependence for the chemical shift of: (a) DNB multiplet and (b) methyl multiplet. The numbers on the curves represent the degree of polymerization of PEG. The empty diamonds represent the methyl signal in dilute (decomplexed) solutions.

out of the CT complex by water, the oxygen donors are getting their electron density back, causing increased shielding on diluting solutions of concentrations smaller than about 17 wt. % (Figure 10, right, and Figure 12). This effect seems to be dominant over the reduction of the ring current effect that is expected to be the result of the decomplexation process. In this regime, dilution is expected to have a small direct (through hydration) effect on the chemical shift of the protons of the already hydrated PEG. Another reason that may contribute to the observed PEG protons shielding on dilution may be the change in the chain conformation discussed previously. A gauche conformer that would have its oxygens pulled out by water would end up having its protons pointing inward, toward the DNB group, where the ring currents are more intense.

The molecular weight resolution allows us to differentiate and compare between the behaviors of species having different PEG chain lengths. In Figure 13, the concentration dependence of the chemical shift is separated by molecular weights. At concentrations higher than about 20 wt. %, the behavior for different fractions shows the same general trend. At concentrations below about 20 wt. %, there are differences between the DNB proton shifts of the short and long chains. Although for the longer chains they show a shallow minimum separating the two concentration regimes, for the short molecules ( $n = 2$  and

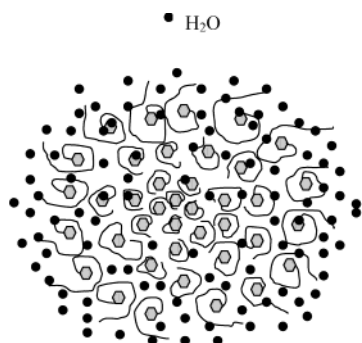


**Figure 14.** Proposed composite aggregate formed by the coiled unimolecular PEG-DNB micelles.

3) the resonances continue to move upfield even below 10 wt. %, indicating a stronger CT involving their aromatic group (Figure 13a). This suggests that for the short chains the hydrophobic effect continue to be dominant at much lower concentrations than for the long-chained analogues. The fact that the short PEG chains continue to collapse onto the DNB group results in their methyl groups being substantially shielded by ring currents. The peaks of oligomers with 2, 3, and 4 EG units for complexed solutions below 10 wt. % are significantly shifted upfield when compared to the peak observed for the methyl protons in dilute (decomplexed) solutions (Figure 13b).

As concentration is increased, in addition to the chemical shift variations, there are several interesting transformations that can be observed with the peaks corresponding to the DNB protons,  $H_{a4}$  and  $H_{a2}$ . The splitting that appears along with the complex formation is very similar to that of observed with the methyl signals, but here it is complicated by J-coupling (Figure 10c and d). However, the aromatic proton signals undergo two other changes in their appearance. First, at a concentration of about 15 wt. % (Figure 10e), the splitting due to J-coupling disappears, and now the aromatic signal contains about the same number of peaks as the methyl signal, but is less spread. The sample at about 15% represents a critical situation, bordering the two concentration regimes described above. Overall, the aromatic protons are most shielded in this solution (Figure 10e) suggesting that most of the fractions form their tightest complexes with a maximum CT from the ether oxygens to the DNB ring. The

same thing is suggested by the maximum observed for the NOESY cross-peak volume (Figure 11) at about same concentration range. The cancellation of the J-coupling means that after CT reaches a certain level, for any given oligomer the protons  $H_{a4}$  and  $H_{a2}$  become magnetically equivalent, showing just one singlet.

Another significant change of the aromatic protons is observed in the high concentration regime. At about 50 wt. %, the multiplet coalesces into a structureless broad signal and at 85 wt. % the signal displays the “normal pattern”, but much broader now, due to the high viscosity of the solution. The chemical shift (Figure 10) and NOESY data (Figure 11) suggest that as concentration increases above 15% the complex may be less tight, probably because there is not enough water to cause the PEG chains collapse onto the hydrophobic DNB. First idea that came to mind was that at very high concentrations, the CT complexes could be more dynamic and probably significantly intermolecular in nature, causing coalescence and broadening of the NMR signals. But this would not explain why the methyl signal does not coalesce, even at very high concentration (Figure 10) and why the coalesced signal is actually narrower than the noncoalesced multiplets seen at smaller concentrations. It seems then that the two multiplets, methyl, and aromatic, may be controlled by different phenomena, or the importance of the involved effects may vary from one case to the other. We attempt an explanation in the next section where a model that accounts for both complexation and aggregation is proposed.

**Structural Model for Concentrated Aqueous Solutions of PEG-DNB.** The PEG-DNB molecule has an amphiphilic character, being the “reverse” of a typical surfactant, i.e., it has a hydrophobic DNB head and a hydrophilic PEG tail. The hydrophobic DNB is the reason for the phase separation occurring on dilution and cooling. Some aggregation process may also occur in the one-phase solutions. This aggregation is supported by SAXS measurements and Pulse Field Gradient Spin-Echo (PFG SE) NMR studies,<sup>42</sup> indicating that large aggregates of about 7 to 9 nm are present at concentrations as low as 6.3 wt. %. The size of these aggregates is much larger than the molecular size, suggesting the existence of supramolecular structures. As was reported previously<sup>14</sup> and further demonstrated in this paper, for concentrations higher than about

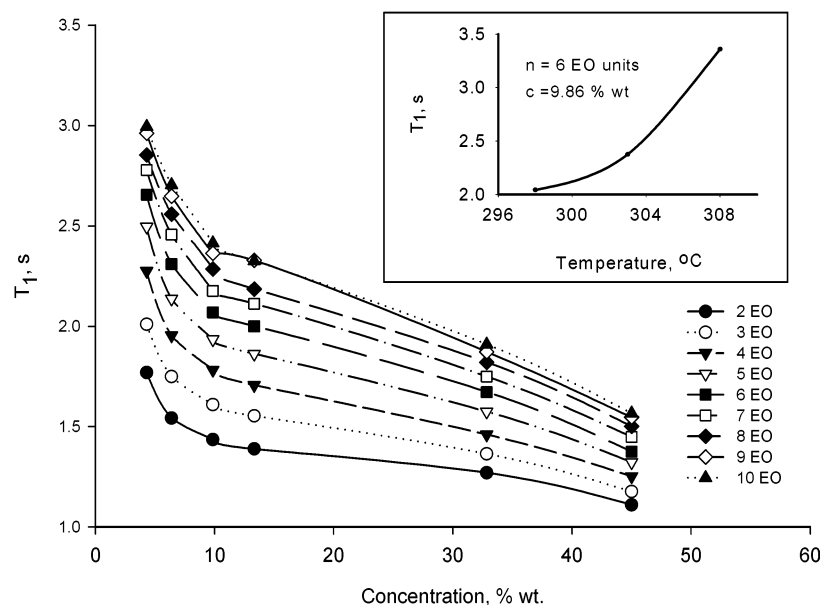


**Figure 15.** Spin-lattice relaxation time of the methyl protons vs concentration for several fractions having various numbers of EO units per PEG chain.



4 wt. %, PEG-DNB maintains a coil conformation with the PEG chain surrounding the DNB group. This means that the aggregates cannot be simple core-shell type, where the core would be made of hydrophobic DNB groups and the shell would consist of PEG chains, for the simple reason that PEG and DNB are stuck together. The only model that can account for the coexistence of aggregation and coiled conformation is a supramicellar composite (multicenter) aggregate (see Figure 14) formed by the association of many PEG-DNB coils, where each of these can be thought of as unimolecular micelles. The shorter the PEG chain the more hydrophobic the molecule, and it will be located closer to the center of the aggregate. A detailed investigation of the aggregation process, including the very dilute solutions, is in progress.<sup>42</sup>

The proposed model is in very good agreement with the molecular weight and concentration dependence of the methyl protons spin-lattice relaxation times,  $T_1$ , (Figure 15). The inset shows the temperature dependence of the  $T_1$  proving the relatively fast regime motion existent in the investigated solutions. This is further supported by the significant decrease in  $T_1$  with the increased concentration when the viscosity of the solution increases. Regarding the molecular weight dependence, the faster relaxation time observed with the shorter chains may seem unexpected because the molecular tumbling should be faster in smaller molecules and make the spin-lattice relaxation less efficient. However, the short chain complexes, preferentially located within the center of the composite aggregate, are experiencing a more rigid hydrophobic local environment than the longer chain molecules, which are expected to be closer to the hydrated and less compact aggregate surface. Therefore, the relaxation of the methyl protons in short chains is more efficient than in the long-chain complexes where the methyl groups enjoy more motional freedom. Further support for the radial distribution of molecular weight fractions is brought by the concentration dependence of  $T_1$ 's in Figure 15, where it can be seen that between 10 and 50 wt. % the decrease in  $T_1$  is less significant for the short chain PEG-DNB. For example, within that concentration range, for  $n = 2$  EO units,  $T_1$  decreases by 15%, whereas for the  $n = 10$  EO units the decrease in  $T_1$  is 29%. The short chain unimers located in the "watertight" center of the supramicellar aggregate barely sense the alteration in hydration and mobility that is associated with change in overall concentration. On the other hand, this change affects drastically the long chain coils located close to the aggregate surface.

The same conclusion can be reached analyzing the concentration dependence of the DNB chemical shift when separated by molecular weights (Figure 13 a). For the long chain molecules there is a shallow minimum marking the border between the hydration- and hydrophobicity-determined regimes. On the other hand, for the very short chains there is no such critical point, even at overall concentrations as low as 6.3 wt. %, which means that within the preponderantly hydrophobic center of the aggregate there is not enough hydration to pull out the PEG chains and cause decomplexation. On the basis of this, the composite aggregate can be characterized by a positive hydration gradient from the center toward the surface, gradient that diminishes along with increasing concentration. The diminishing gradient at high concentrations is best visualized when comparing the distribution of  $T_1$  values at high concentrations ( $\Delta T_1 = 0.5$  s at 45 wt. %) and low concentrations ( $\Delta T_1 = 1.2$  s at 4.3 wt. %) (Figure 15). The hydration gradient is the result of the hydrophobicity gradient associated with the distribution of the molecular weight fractions along the aggregate radii.

Using the composite aggregate model, we are now able to explain the collapse of the DNB multiplet at about 50 wt. %. All of the similarities between the DNB and methyl multiplets suggest that they have at least one common phenomenon between them: charge transfer complexation. But, in addition to that, there has to be some process that affects the aromatic multiplet resolution, while it has less influence on the methyl multiplet. Its effect on multiplet resolution should disappear at concentrations around 50 wt. %, when the aromatic multiplet is seen to collapse, while the resolution of the methyl multiplet is practically unchanged. We believe that for the DNB multiplet, in addition to complexation-related effects, there might be ring current effects from the neighboring DNB rings inside the aggregate, which, for packing reasons, may tend to have a coplanar orientation. The presence of the PEG chains side-wise to the DNB rings should not prevent the coplanar orientation, although it may alter the distance between the neighboring rings. If this is true, then the shorter the chain, the closer the neighboring rings would be, and the more shielded the corresponding aromatic protons. This means that this aromatic stacking can increase the molecular weight selectivity of the chemical shift and have a major impact on the resolution of the DNB multiplet, causing a signal spreading. Furthermore, the hydration gradient within the aggregate probably causes a gradient of packing density as well. The side-wise orientation of the PEG chains probably keeps them far enough from the ring currents of the neighboring DNBs, which means that the resolution of the methyl multiplet is mostly determined by the intramolecular complexation effects and less by aromatic stacking. It then seems reasonable to assume that if the aggregate structure or its packing density gradient is disrupted, the aromatic stacking is also disrupted and the DNB multiplet will suffer a significant resolution loss, while the methyl multiplet resolution should be less affected. It is known that in oxyethylene based surfactant solutions at high concentrations, the aggregates start overlapping and the exchange of unimers becomes very important causing the aggregates to gradually merge and form less defined surfactant continuous domains.<sup>41</sup> It has also been found that increasing the surfactant concentration broadens the aggregate size distribution.<sup>43</sup> Furthermore, considering the composite aggregate model, it is very probable that the diminishing hydration gradient will reduce the packing density gradient and, therefore, the molecular weight resolution. This state produces a featureless DNB peak at high concentrations.

The combination of aromatic stacking disruption and weakening of the intramolecular charge-transfer results in the aromatic signal regenerating its two-peak structure (corresponding to  $H_{a2}$  and  $H_{a4}$ ) at very high concentrations (Figure 10g). The doublet and triplet structures of these peaks are not visible anymore due to viscosity-induced broadness of the NMR lines. The weakening of charge-transfer reduces the resolution of the methyl multiplet, its chemical shift range shrinks from 0.2 ppm at 50 wt. % to about 0.13 ppm at 85 wt. % (Figure 10f and g). However, the methyl multiplet still retains a higher molecular weight resolution than the methyl signal of the dilute solutions (Figure 10a and b), suggesting that the molecules still form coil complexes, although the charge transfer from PEG to DNB is significantly reduced.

## Conclusions

A sample of poly(ethylene glycol) [PEG] capped with a methyl ether at one end and a 3,5-dinitrobenzoate (DNB) ester at the other forms intramolecular charge-transfer complexes. The DNB group is a good  $\pi$ -electron acceptor while the oxygen



atoms from the polyether chain can act as  $p$ -electron donors.<sup>19</sup> The strongest complexes are formed in relatively concentrated aqueous solutions, where the hydrophobicity of the DNB group favors the coiled conformation required by the CT complex. In dilute aqueous solutions, the PEG chains are stretched out of the CT complex by hydration, which overcomes both the hydrophobic effect and CT interactions. The complex destruction leaves the hydrophobic DNB group exposed to water, and a liquid–solid-phase separation occurs. The same kind of phase separation can be induced by cooling, and it is connected to the increase in  $-C-C-$  gauche conformer population.<sup>32,33,34</sup> In addition to the solid–liquid-phase separation at low temperature, a liquid–liquid-phase separation, common feature for aqueous solutions containing oxyethylene compounds, is observed at higher temperatures. The results presented here are in good agreement with the conformational models<sup>21,33</sup> explaining the temperature induced phase separation in aqueous solutions of poly(ethylene glycol)s.

One of the most interesting consequences of the CT complexation is the unusual multiplet pattern observed in <sup>1</sup>H NMR spectra of the concentrated aqueous solutions. The complexation acts as a chemical shift reagent, allowing resolution by molecular weight<sup>14</sup> for the methyl and aromatic signals of PEG-DNB. The molecular weight selectivity of the chemical shift is related to the different conformations adopted by complexes having different PEG lengths, these conformations being the result of the competition between hydration forces on one hand, and CT interactions and hydrophobicity of DNB on the other. In terms of NMR chemical shifts, the result of this competition affects the balance between the three interactions affecting the proton shielding: CT, ring currents and hydration. Stronger CT complexes are formed by the low-molecular weight PEG-DNB where the shorter PEG chains are less hydrated and significantly shielded by ring currents. On the other hand, for the more hydrophilic higher molecular weight PEG-DNBs, the longer the PEG chain the stronger are the stretching forces exerted by hydration and the weaker the CT interactions and the ring currents. The resolution of the DNB multiplet is affected not only by intramolecular complexation but also by the ring currents coming from the neighboring rings within the large aggregates suggested by NMR and SAXS.<sup>42</sup> The effect of aromatic stacking fades at concentrations higher than 50 wt. %. A supramolecular composite (multicenter) aggregate (see Figure 14) formed by the association of unimolecular coil-like micelles has been suggested. Within this aggregate the more hydrophobic short chain complexes form the core part while the more hydrophilic long chain complexes will be preferentially situated closer to the surface where hydration is more effective.

The weak ring currents observed here suggest that the PEG chain is situated on the side of the DNB ring, allowing for an optimum orbital interaction between  $p$ -orbitals from oxygen and  $\pi$ -orbitals from the DNB. This conformation also allows aromatic stacking in the aggregates. At very high concentrations, the aromatic stacking disruption and weakening of the intramolecular charge cause the molecular weight resolution to be totally lost for the aromatic protons but partially retained for the methyl protons. The loss in resolution is also caused to some extent by the increase in the solution viscosity.

**Acknowledgment.** We thank NSERC Canada for financial support. A. N., Canada Research Chair in Polymer Chemistry, acknowledges the CRC Program of the Government of Canada. G.C. acknowledges the PGS B Scholarship granted by NSERC.

## References and Notes

- (1) Jonsson, B.; Lindman, B.; Holmberg, K.; Kronberg, B. *Surfactants and Polymers in Aqueous Solution*; John Wiley & Sons: Chichester, 1998, p 91.
- (2) Point, J. J.; Jasse, B.; Dosière, M. *J. Phys. Chem.* **1986**, *90*, 3273.
- (3) Point, J. J.; Coutelier, C. *J. Polym. Sci., Polym. Phys. Ed.* **1985**, *23*, 231.
- (4) Harris, D. J.; Bonagamba, T. J.; Hong, M.; Schmidt-Rohr, K. *Macromolecules* **2000**, *33*, 3375.
- (5) Paternostre, L.; Damman, P.; Dosière, M. *Macromolecules* **1997**, *30*, 3946.
- (6) Spváek, J.; Paternostre, L.; Damman, P.; Draye, A. C.; Dosière, M. *Macromolecules* **1998**, *31*, 3612.
- (7) Wright, P. W. In *Polymer Electrolytes*; MacCallum, J. R., Vincent, C. A., Eds.; Elsevier Applied Science: London, 1989, vol. 2, chapter 3.
- (8) von Helden, G.; Wyttenbach, T.; Bowers, M. T. *Science* **1995**, *267*, 1483.
- (9) Besner, S.; Valee, A.; Bouchard, G.; Prud'homme, J. *Macromolecules* **1992**, *25*, 6480.
- (10) Mayer, W. H. *Adv. Mater.* **1998**, *10*, 439.
- (11) Andrews, L. J.; Keefer, R. M. *J. Org. Chem.* **1988**, *53*, 537.
- (12) Kwei, T. K.; Nishi, Roberts, R. F. *Macromolecules* **1974**, *7*, 667.
- (13) Natansohn, A. *Polym. Adv. Technol.* **1994**, *5*, 133.
- (14) Cojocariu, G.; Natansohn, A. *Macromolecules* **2001**, *34*, 3827.
- (15) Jeneer, J.; Meier, B. H.; Bachmann, P.; Ernst, R. R. *J. Chem. Phys.* **1979**, *71*, 4546.
- (16) Wagner, R.; Berger, S. *J. Magn. Reson.* **1996**, *123* A, 119.
- (17) Marion, D.; Wuthrich, K. *Biochem. Biophys. Res. Commun.* **1983**, *113*, 967–974.
- (18) Vold, R. L.; Waugh, J. S.; Klein, M. P.; Phelps, D. E. *J. Chem. Phys.* **1968**, *48*, 3831.
- (19) Foster, R. *Organic Charge-Transfer Complexes*, Academic Press: London, 1969, p 4.
- (20) Goldstein, R. E. *J. Chem. Phys.* **1984**, *80*, 5340.
- (21) Karlström, G. *J. Phys. Chem.* **1985**, *89*, 4962.
- (22) Kjellander, R.; Florin, E. *J. Chem. Soc., Faraday Trans.* **1981**, *77*, 2053.
- (23) Matsuura, H.; Sagawa, T. *J. Mol. Liq.* **1995**, *65/66*, 313.
- (24) Masatoki, S.; Takamura, M.; Matsuura, H.; Kamogawa, K.; Kitagawa, T. *Chem. Lett.* **1995**, 991.
- (25) Tasaki, K. *J. Am. Chem. Soc.* **1996**, *118*, 8459.
- (26) Tasaki, K. *Macromolecules* **1996**, *29*, 8922.
- (27) Begum, R.; Matsuura, H. *J. Chem. Soc., Faraday Trans.* **1997**, *93*, 3839.
- (28) Becker, E. D. *High-Resolution NMR. Theory and Chemical Applications*; Academic Press: San Diego, 2000, p176.
- (29) Connor, T. M.; McLauchlan, K. A. *J. Phys. Chem.* **1965**, *69*, 1888.
- (30) Takahashi, Y.; Tadokoro, H. *Macromolecules* **1973**, *6*, 672.
- (31) Harren, A. H. *J. Chem. Phys.* **1972**, *56*, 5681.
- (32) Matsuura, H.; Fukuhara, K. *J. Mol. Struct.* **1985**, *126*, 251.
- (33) Andersson, M.; Karlström, G. *J. Phys. Chem.* **1985**, *89*, 4957.
- (34) Smith, G. D.; Bedrov, D.; Borodin, O. *J. Am. Chem. Soc.* **2000**, *122*, 9548.
- (35) Sun, D.; Chen, J.; Lu, W.; Zheng, X. *J. Sol. Chem.* **1998**, *27*, 1097.
- (36) Haigh, C. W.; Mallion, R. B. *Prog. NMR Spectrosc.* **1980**, *13*, 303.
- (37) Liu, K.-J.; Parsons, J. L. *Macromolecules* **1969**, *2*, 529.
- (38) Donato, I. D.; Magazu, S.; Maisano, G.; Majolino, D.; Migliardo, P.; Pollicino, A. *Mol. Phys.* **1996**, *87*, 1463.
- (39) Matsuura, H.; Fukuhara, K. *Bull. Chem. Soc. Jpn.* **1986**, *59*, 763.
- (40) Maconnachie, A.; Vasudevan, P.; Allen, G. *Polymer* **1978**, *19*, 33.
- (41) Nilsson, P.-G.; Wennerström, H.; Lindman, B. *J. Phys. Chem.* **1983**, *87*, 1377.
- (42) Cojocariu, G.; Natansohn, A.; Singh, M., manuscript in preparation.
- (43) Walderhaug, H.; Hansen, F. K.; Abrahmsen, S.; Persson, K.; Stilbs, P. *J. Phys. Chem.* **1993**, *97*, 8336.